Veterinary Research

Dysregulated microRNAs in blood correlate with central nervous system neuropathology of prion disease

Sonia Pérez-Lázaro[1,2,3*] , Inmaculada Martín-Burriel[1,2,3,4,5], Luca Cozzuto[6], Julia Ponomarenko[6,7], Juan J. Badiola[1,2,3], Rosa Bolea[1,2,3] and Janne M. Toivonen[2,3,4,5]

Abstract

The role of microRNAs (miRNAs) in neurodegenerative diseases has gained significant attention because of their involvement in gene regulation and potential as biomarkers. In prion diseases, including scrapie, miRNAs may modulate pathogenesis and disease progression. This study investigated circulating miRNA profiles in the blood of sheep naturally affected by scrapie at preclinical and clinical stages using small RNA sequencing and RT-qPCR validation. While only one novel miRNA was dysregulated in preclinical blood samples, 66 previously annotated miRNAs were significantly dysregulated in clinical sheep compared with healthy sheep. These miRNAs are associated with pathways commonly altered in neurodegenerative diseases, such as autophagy, ubiquitin-mediated proteolysis, and endoplasmic reticulum protein processing. Notably, miR-1271-5p, let-7f-5p, miR-186-5p, and miR-425-5p were consistently upregulated in the central nervous system of clinical animals, replicating the results observed in blood, with an increasing trend already in the preclinical stage and a strong correlation with neuropathological prion features. Additionally, predicted target genes such as *UBQLN2*, *PGK1*, *KRAS*, and *CLTC* were inversely expressed relative to these miRNAs, supporting their regulatory roles. These findings highlight the relevance of circulating miRNAs in prion neuropathology and support further research into the specific functional roles of these miRNAs and their predictive capacity for disease progression.

Keywords Prion, neurodegenerative diseases, scrapie, microRNA, biomarkers

---

*Correspondence:
Sonia Pérez-Lázaro
soniperez97@gmail.com
[1] Centro de Encefalopatías y Enfermedades Transmisibles Emergentes (CEETE), Facultad de Veterinaria, Universidad de Zaragoza, Zaragoza, Spain
[2] Instituto Universitario de Investigación Mixto Agroalimentario de Aragón (IA2) UNIZAR-CITA, Zaragoza, Spain
[3] Instituto de Investigación Sanitaria de Aragón (IIS-Aragón), Zaragoza, Spain
[4] Laboratorio de Genética Bioquímica (LAGENBIO), Facultad de Veterinaria, Universidad de Zaragoza, Zaragoza, Spain
[5] Centro de Investigación Biomédica en Red de Enfermedades Neurodegenerativas (CIBERNED), Instituto de Salud Carlos III, Madrid, Spain
[6] Centro de Regulación Genómica (CRG), The Barcelona Institute of Science and Technology (BIST), Barcelona, Spain
[7] Universitat Pompeu Fabra (UPF), Barcelona, Spain

Pérez-Lázaro *et al. Veterinary Research*   (2025) 56:132

Page 2 of 18

Introduction

Prion diseases, also known as transmissible spongiform encephalopathies (TSEs), represent a group of complex neurodegenerative conditions that affect both animals and humans. These disorders are caused by a misfolded protein (PrP^{Sc}), which acts as an infectious agent by inducing the abnormal folding of the physiological cellular prion protein (PrP^{C}). PrP^{C}, encoded by the *PRNP* gene, is highly expressed in the brain and plays a role in protection against oxidative stress, synaptic transmission and neuronal homeostasis [1]. However, its conversion into PrP^{Sc} causes the formation of non-degradable aggregates and their accumulation, primarily in the central nervous system (CNS). The deposition of these aggregates leads to progressive neurodegeneration and neuronal damage, ultimately resulting in the death of the individual. Common neuropathological findings in the CNS include PrP^{Sc} deposits, spongiform vacuolation and activation of astrocytes and microglia [2]. Animal prion diseases include scrapie in sheep and goats, the first TSE described, bovine spongiform encephalopathy in cattle and chronic wasting disease (CWD) in cervids. In humans, Creutzfeldt–Jakob disease is the most prevalent disease, with its sporadic nature (sCJD) accounting for most cases [3]. In addition to prion diseases, a group of neurodegenerative pathologies commonly called prion-like disorders are characterised by the accumulation of protein aggregates, such as beta-amyloid and tau in Alzheimer's disease (AD), alpha-synuclein in Parkinson's disease (PD) and SOD1 and TDP-43 in amyotrophic lateral sclerosis (ALS) [4, 5].

While the pathological hallmarks of prion diseases are well documented, the molecular mechanisms underlying the onset and progression of these diseases, especially during the asymptomatic preclinical stage, remain poorly understood. Early detection before the appearance of clinical signs is essential for understanding disease progression.

Currently, the detection of PrP^{Sc} in post-mortem brain tissue is the only definitive method for the diagnosis of prion diseases. In classical scrapie, however, preclinical diagnosis is possible in vivo through rectal mucosa biopsies because of the spread of PrP^{Sc} throughout the lymphoid tissue at the beginning of the pathogenesis of the disease [6]. Although this technique is not 100% sensitive for diagnostic use, as the involvement of the lymphoid system depends on many factors, it is fully specific and provides us with an animal model of natural prion disease in which to investigate all the molecular changes occurring in the preclinical stage. In this context, sheep scrapie has previously been used as a faithful model for human prion diseases [7, 8].

In recent years, microRNAs (miRNAs) have emerged as key regulators of numerous diseases. These small (20–25 base pairs long), noncoding nucleotides can regulate gene expression post-transcriptionally, binding to complementary messenger RNA (mRNA) sequences through the RNA-induced silencing complex (RISC) and thus degrading, destabilising or translationally inhibiting target mRNAs [9]. It is predicted that approximately 70% of the identified miRNAs are expressed in the brain and that they may regulate up to 30% of protein-coding genes [10, 11]. The expression and regulatory potential of these genes suggest that they may play important roles in the pathogenesis of neurodegenerative disorders, including prion diseases.

Particularly in prion diseases, previous research has identified several miRNAs that may directly regulate *PRNP* expression, and moreover, the prion protein has also been predicted to interact with miRNA biogenesis pathways [12]. Possibly related to this direct regulation, Norsworthy and colleagues identified a miRNA signature capable of differentiating sCJD from AD, although these miRNAs did not correlate with clinical parameters or disease progression [13]. These findings indicate that further research is needed to understand the functional role of these proteins in the neuropathogenesis of prion diseases. Studies using small RNA sequencing in the CNS of preclinical murine models of prion disease have revealed that only a limited number of miRNAs are altered in early stages, suggesting that miRNA dysregulation may occur in advanced stages of the disease [14, 15]. In naturally occurring scrapie, research has been limited to specific miRNAs and has focused only on the clinical stage of disease, leaving unanswered what happens in naturally occurring disease before the onset of clinical signs or whether the expression of miRNAs correlates with prion neuropathology [16, 17].

Interestingly, miRNAs exhibit remarkable stability in body fluids, such as blood and cerebrospinal fluid (CSF), due to their encapsulation in extracellular vesicles or their association with RNA-binding proteins, making them ideal fluid biomarkers [9, 18]. Blood is a highly accessible and minimally invasive body fluid, offering significant advantages for early diagnosis and disease monitoring. miRNAs detected in blood often originate from various tissues, potentially providing insights into otherwise inaccessible brain pathologies [19]. Nevertheless, only one study in a prion murine model has identified commonly dysregulated miRNAs between body fluids and the CNS, highlighting the need for further research to identify reliable biomarkers in peripheral fluids that could reflect what is happening in the brain during disease progression [20].

Pérez-Lázaro *et al. Veterinary Research*   (2025) 56:132

Page 3 of 18

In this study, we aimed to investigate whether miRNA dysregulation in blood could serve as a biomarker for disease progression, with a specific focus on a natural model of prion disease. We also sought to test the hypothesis that miRNA dysregulation appears predominantly in the clinical stages, as suggested by prior studies in murine prion models. Given these objectives, we performed next-generation small RNA sequencing to profile, for the first time, miRNA changes in blood from healthy sheep through preclinical and clinical stages of naturally affected scrapie sheep. After validating significantly dysregulated miRNAs in the blood via real-time quantitative PCR (RT-qPCR), we also analysed these miRNAs in the CNS and correlated their expression with the characteristic neuropathology of prion diseases. Furthermore, we investigated the expression of potential mRNA targets of dysregulated miRNAs to gain insights into their role in neurodegeneration.

Materials and methods
Animals
A total of 25 female Rasa Aragonesa sheep (3–6 years old), which carry the ARQ/ARQ *PRNP* genotype, one of the most prevalent *PRNP* genotypes in scrapie-affected Rasa Aragonesa sheep [21], were included in this study. These sheep were categorised into three groups according to their scrapie-affection status and disease progression: 10 healthy sheep, 5 naturally scrapie-affected sheep in the preclinical stage displaying no clinical signs and 10 scrapie-affected sheep in the clinical stage of the disease. All sheep were bred under natural flock conditions, and it is expected that their reproductive status would be similar across groups. None of the animals were lactating at the time of sampling. Body condition scores were assessed using a standard 1–5 scale (1 = very thin; 5 = obese) by palpation of the lumbar region, with values ranging from 2.5 to 3.5 in healthy and preclinical animals. Healthy animals were used as the control group and were from healthy flocks with no previous scrapie cases. Animals naturally affected with scrapie were selected from flocks involved in scrapie outbreaks. Specifically, clinical sheep were identified by characteristic scrapie clinical signs such as pruritus coursing with alopecic areas around the lumbar region, cachexia -with body condition scores ranging from 1.5 to 2.25, consistent with disease progression- and ataxia [22], and confirmed by the detection of PrP^{Sc} deposits in CNS samples using immunohistochemistry (IHC), as detailed in the histopathological and immunohistochemical analyses section below. Furthermore, preclinical animals with no clinical signs were detected by large-scale rectal mucosa biopsies and subsequent IHC, as described elsewhere [23].

Blood and brain tissue sample collection
Blood samples (2.5 mL) were collected by jugular vein puncture into PAXgene Blood RNA Tubes (PreAnalytiX, Switzerland) to better preserve intracellular RNA for molecular procedures. The tubes were filled, inverted 10 times and, after two hours at room temperature (RT), frozen at −80 °C until processing. The animals were subsequently sacrificed via intravenous injection of sodium pentobarbital, followed by exsanguination. Samples from two areas of the CNS (medulla oblongata at the level of the obex and thalamus) were divided in half sagittally; one half was finely minced and preserved in RNAlater Solution (Invitrogen, USA) at −80 °C for posterior RNA extraction, while the other half was fixed in 10% formaldehyde for histopathological and immunohistochemical analyses.

Histopathological and immunohistochemical analyses
Formalin-fixed obex and thalamus tissues were paraffin-embedded, sliced into 4 µm thick sections and dried at 37 °C for 24 h. Haematoxylin and eosin (HE) staining was performed to assess neuropathological changes and spongiosis degeneration. PrP^{Sc} deposits in the CNS were quantified by IHC with an L42 antibody (1/500, R8005, R-Biopharm, Germany) following an established protocol [24]. Astrogliosis and microgliosis were also evaluated by IHC, using glial fibrillary acidic protein (GFAP; 1/500, Z0334, Dako, Denmark) as an astrocyte marker and ionised calcium-binding adaptor molecule 1 (Iba1; 1/1000, 019-19741, Wako, USA) as a microglial marker. Previously reported protocols were followed for both [25]. Blinded histopathological and immunohistochemical evaluations were performed using a Zeiss Axioskop 40 optical microscope (Zeiss, Germany). Microphotographs of representative areas of each region (thalamus: dorsal, central, ventral; medulla oblongata at the level of the obex: cuneate nucleus, dorsal motor nucleus of vagus, inferior olive) were taken using an Axiocam 305 color camera (Zeiss, Germany) and Zeiss Zen v3.9 software, ensuring the same intensity and contrast settings across all samples. The staining intensity was analysed via ImageJ v1.54 g software with the Colour Deconvolution 2 v2.1 plugin [26], following a previously described method [27]. Briefly, colour deconvolution vectors appropriate for each staining type (H DAB for IHC or H&E for HE) were selected accordingly, and a specific threshold was set manually to remove background signals and uniformly applied to each neuropathological feature for consistency across samples. The mean grey values were then measured and averaged by area and sample for statistical analysis and graphical representation. In the IHC samples, higher mean grey values indicated greater

Pérez-Lázaro *et al. Veterinary Research*   (2025) 56:132

Page 4 of 18

staining intensity, corresponding to higher expression of the proteins marked, whereas in the HE-stained samples, a higher mean grey value reflected greater spongiosis.

Total RNA extraction

Total RNA was extracted from the entire volume of whole blood collected using the PAXgene Blood RNA Kit (PreAnalytiX, Switzerland) following the manufacturer's steps. Eighty microliters of RNA was obtained and stored at -80 °C until use. A Direct-zol RNA Miniprep Plus Kit (Zymo Research, USA) was used for RNA extraction from obex and thalamus preserved tissues. Twenty milligrams of tissue was homogenised in 1 mL of TRI Reagent (Zymo Research, USA) using TeSeE grinding tubes and a TeSeEPrecess 48 homogeniser (Bio-Rad, USA). After the samples were left for 5 min at 4 °C and for another 5 min at RT, chloroform phase separation was performed by adding 200 μL of chloroform, shaking for 15 s, incubating for 3 min at RT and centrifuging at 12 000 *g* at 4 °C for 15 min. After this, the colourless upper aqueous phase was mixed with an equal volume of ethanol and transferred into the kit columns. The manufacturer's protocol was followed from this point onwards for RNA purification. The RNA was eluted with 50 μL of nuclease-free water and stored at −80 °C until analysis.

Small RNA sequencing

RNA quality control and concentration measurements were performed using a NanoDrop spectrophotometer (Thermo Fisher Scientific, USA) and a 2100 Bioanalyzer (Agilent, USA). All the RNA integrity number (RIN) values were above 8. Blood RNA samples were sent to the Genomics Unit at the Centro de Regulación Genómica (CRG, Barcelona, Spain), where small RNA sequencing was performed. The sequencing libraries were prepared using the NEBNext Multiplex Small RNA Library Prep Set for the Illumina Kit (New England Biolabs, USA) following the manufacturer's protocol. Fifty bp (base pairs) single-end reads were sequenced on the Illumina HiSeq 2500 platform (Illumina, USA).

Bioinformatic data analysis

The raw reads were quality-checked using FastQC v0.11.7 [28] to assess the read quality, adapter contamination and GC content. Sequencing adapters and reads for quality and length were trimmed using Skewer v0.2.2 [29], with default parameters. Reads between 15 and 30 bases in length were aligned to the sheep reference genome (Oar_v4.0) using ShortStack v3.8.5 [30], which is based on Bowtie 1 v1.2.2 [31]. MiRNAs were annotated using *Ovis aries* miRNAs in miRBase v22 [32], and reads were quantified using HTSeq-count [33]. Owing to the limited number of *Ovis aries*

miRNAs in miRBase, a high percentage of reads were not assigned. These reads were subjected to de novo prediction using Infernal v1.1.4 [34] with the whole Rfam database v14.6 [35], preselecting miRNAs with at least ten reads across all samples. Additionally, miR-Deep2 v2.0.1.2 [36] was employed to detect mature miRNAs from other species available in miRBase, and to predict novel miRNAs. The secondary structure of novel miRNAs was predicted using RNAfold from the ViennaRNA package v2.0 [37], and the minimum folding energy (MFE) of the structure was evaluated against a distribution obtained by shuffling input sequences while preserving dinucleotide composition, using RANDfold [38].

Infernal and miRDeep2 predictions were combined with the annotated miRNAs in *Ovis* arrays from miR-Base and filtered to remove redundancy using Bedtools v2.27.1 [39] to generate a final annotation. Merged annotation reads were quantified using HTSeq-count and filtered to retain miRNAs with at least one read per sample per group. Specifically, miRNAs were retained if they had at least ten reads in the clinical and healthy groups each and five reads in the preclinical group. Differential expression analysis was performed using DESeq2 v1.34 [40]. Sequences from differentially expressed novel miR-NAs were queried against the RumimiR database [41] using the integrated BLAST tool to evaluate whether any of those miRNAs had been previously reported in other ruminant studies. We considered only those hits with an E value lower than 0.001 to be highly accurate, and priority was given to sheep studies, all of which used the same reference sheep genome, Oar_v4.0, when available.

Unsupervised multivariate analysis was conducted using principal component analysis (PCA) in R v4.2.2, with the ggfortify v0.4.16 package, to assess the small RNA sequencing data distribution across the three experimental groups on the basis of logarithmically transformed read counts. A Venn diagram was created using the VennDiagram v1.7.3 R package, and volcano plots were designed with the ggplot2 v3.4.2 R package. Additionally, hierarchical clustering analysis was performed using the ComplexHeatmap v2.14.0 R package. Fold change (FC) values were calculated from selected miRNA logarithmically transformed read counts, referring each scrapie-affected stage to the mean of the healthy group. Z scores were calculated by scaling FC values, and hierarchical clustering was conducted using Euclidean distance and a complete linkage method. Functional enrichment analysis based on the Kyoto Encyclopedia of Genes and Genomes (KEGG) pathways was performed using DIANA-miRPath v4.0 [42], which uses human databases for target prediction with TarBase v8.0, and the union merging method for genes was selected.

Pérez-Lázaro *et al. Veterinary Research*   (2025) 56:132

Page 5 of 18

miRNA RT-qPCR analyses

For both blood and CNS samples, complementary DNA (cDNA) was synthesised using the TaqMan MicroRNA Reverse Transcription Kit (Thermo Fisher Scientific, USA) following the manufacturer's instructions. Thirty nanograms of RNA was used as a template, and two reverse transcription reactions were performed, pooling separately TaqMan MicroRNA RT Assays (Thermo Fisher Scientific, USA) for the miRNAs of interest and for potential housekeeping miRNAs and adding two negative controls with no reverse transcriptase or no template to test the reaction.

RT-qPCR was performed on a QuantStudio 3 instrument (Thermo Fisher Scientific, USA). Reactions were run in triplicate and consisted of 5 µL of TaqMan Fast Universal Master Mix (2X) without AmpErase UNG (Thermo Fisher Scientific, USA), 4.5 µL of 1/5-diluted cDNA and 0.5 µL of TaqMan MicroRNA TM Assays (Thermo Fisher Scientific, USA) for each miRNA analysed. Housekeeping miRNA candidates were selected from the blood small RNA sequencing data. Additionally, sn-U6 was analysed as a potential housekeeping gene only in the CNS because of its previously reported stability in this type of sample [14]. The TaqMan probe references are detailed in Additional file 1. Cycle threshold (Ct) values were calculated using the QuantStudio Design & Analysis software v1.5.3 (Thermo Fisher Scientific, USA), and Ct values below 35 were considered acceptable. Blood and obex samples were normalised to the mean of miR-92a and miR-328, whereas thalamic samples were normalised to the mean of sn-U6, miR-320 and miR-328, identified as the most stable miRNAs among groups by RefFinder [43], with no significant Ct differences across groups (Additional file 2). For RT-qPCR results analysis, the $2^{-\Delta\Delta Ct}$ method was used, with the healthy control group used as the reference group [44]. Briefly, delta Ct values were calculated by subtracting the mean housekeeping Ct values from the selected miRNA Ct values for each sample. The mean of the delta Ct values of all healthy controls was subsequently subtracted from each sample to obtain the delta Ct values, and the calculated $2^{-\Delta\Delta Ct}$ values were graphed as individual dots.

miRNA target identification and expression analyses

Since there are no sheep-specific miRNA target databases, human databases were used after confirming miRNA sequence conservation. Target genes for selected miRNAs likely to be involved in prion pathology were evaluated using TarBase v9.0 [45], considering high-confidence miRNAs with primary interactions only, and filtering for genes validated by a luciferase assay and those validated by immunoprecipitation in more than 5 experiments; miRDB v6.0 [46], filtering results with a target prediction score higher than 80; and DIANA-miRPath v4.0 [42], preselecting target genes related to neurodegenerative pathways. Then, intersections between these databases were performed to refine the target genes. Additionally, two previous articles that used microarrays and mass spectrometry analyses for identifying biomarkers in sheep naturally affected with scrapie were also considered [47, 48] and filtered for genes or proteins inversely expressed to the miRNAs selected. We confirmed the conservation of miRNA–target gene binding sites in sheep, using the alignment comparative genomics tool in Ensembl [49].

For gene expression quantification by RT-qPCR, 1 µg of total RNA was reverse transcribed into cDNA using the qScript cDNA SuperMix Kit (Quantabio, USA) according to the manufacturer's instructions. Primers were designed using Primer3Plus v3.3.0 [50] and PrimerBLAST [51] tools, ensuring separation by an intron when possible, total specificity for the gene in *Ovis aries* and minimal secondary structures between primers. The primers were then tested for their ideal concentration and efficiency, with 90–110% efficiency. *GAPDH*, *G6PD* and *SDHA* were analysed as potential housekeeping genes for their previously reported stability in the CNS of scrapie-affected sheep [52]. The primer sequences and concentrations used are detailed in Additional file 3.

RT-qPCR was performed in triplicate on a QuantStudio 3 instrument (Thermo Fisher Scientific, USA) with the following reaction mixture: 5 µL of RealQ Plus 2×Master Mix Green, low ROX (Ampliqon, Denmark), variable primer concentration (as shown in Additional file 3) and 15 ng of cDNA. Standard run mode was used, with a melt curve used to check for specific amplification. The target gene data in both the obex and thalamus areas were normalised to the means of *G6PD* and *SDHA* because of their better stability, as reported by RefFinder, and their lack of significant differences in Ct values between groups (Additional file 4). The delta Ct values were calculated, and the $2^{-\Delta\Delta Ct}$ method was subsequently used as described for the miRNAs.

Statistical analyses

All the statistical analyses and graphical representations were performed in R version 4.2.2.

Small RNA sequencing *p* values were adjusted (adj *p* value) via Benjamini–Hochberg false discovery rate (FDR) correction for multiple testing. For statistical comparisons between groups, we first used the Shapiro–Wilk test to check data normality. If the data were normal, and after testing for homogeneity of variance with Levene's test, the variables were compared using one-way ANOVA, followed by the Tukey HSD test for multiple pairwise comparisons. Non-normally distributed

Pérez-Lázaro *et al. Veterinary Research*   (2025) 56:132

Page 6 of 18

or non-homogeneous variables were tested using the Kruskal–Wallis test, followed by Dunn's test for multiple pairwise comparisons. Normally distributed variables are described as the mean ± standard deviation, and non-normally distributed variables are described as the median ± interquartile range. For the correlation analysis between miRNA expression levels in the CNS and neuropathological changes, the cor R function and the Hmisc v5.1.1 R package were used for the calculation of Spearman's rank correlation coefficients and correlation p values, respectively. This analysis was performed separately for each CNS area, using the $2^{-\Delta\Delta Ct}$ values for miRNA expression and the ImageJ mean grey value scores for neuropathology.

Data visualisation was conducted using the ggplot2 package in R, and statistically significant differences are indicated in the plots by symbols, where tendencies are marked with ^ (p value < 0.1) and significant results with asterisks: * (p value < 0.05), ** (p value < 0.01) and *** (p value < 0.001).

Results

Neuropathological features of naturally occurring scrapie stages

First, we analysed the characteristic neuropathological features of prion diseases in all the samples included in this study: 5 preclinical naturally scrapie-affected sheep, 10 clinical scrapie sheep and 10 healthy animals (Figure 1). PrP^{Sc} deposits, spongiosis (HE staining), astrogliosis (GFAP) and microgliosis (Iba1), were evaluated in two areas of the CNS previously reported to be the most affected by scrapie: the medulla oblongata at the level of the obex and the thalamus [53]. Similar pathological differences between groups were observed in both CNS regions, with the obex showing greater intensity of these neuropathological features appearing to be more affected. PrP^{Sc} deposits and spongiosis are absent in healthy animals, as these are hallmark features of prion diseases, and both are significantly elevated in scrapie-affected animals and are already altered in the preclinical stage of disease. GFAP and Iba1 reactivity was also significantly increased in clinical animals in both CNS areas studied. Additionally, these markers tended to be more highly expressed in preclinical sheep than in healthy animals, particularly in the obex, whereas in the thalamus, only GFAP displayed early upregulation.

Small RNA sequencing reveals notable miRNA dysregulation in scrapie blood

Next-generation sequencing was performed on blood samples from naturally affected scrapie animals and healthy controls to measure miRNA expression and detect potential differences between diseased and healthy animals. All the samples yielded an average of 6.9 million quality-controlled reads (ranging from 4.4 to 9.4 million reads per sample). The initial analysis aligned almost 96% of the total reads to the sheep reference genome and focused on known miRNAs annotated in the miRBase for sheep. However, the percentage of reads assigned to known miRNAs from sheep was notably low, with a mean assignment rate of less than 3%. Consequently, we used de novo prediction of miRNAs, assigning, on average, almost 90% of the reads to the predicted miRNAs across samples. As a result, 1097 putative miRNAs were identified. After filtering for minimum expression, a total of 670 miRNAs remained. Figure 2A shows the distribution of these miRNAs identified by three bioinformatic tools. Approximately 80% of the miRNAs were identified uniquely by miRDeep2; among these, 106 were detected by miRDeep2 as mature miRBase miRNAs from other species, whereas 452 were predicted as novel miRNAs.

Using these filtered miRNAs, PCA was performed to graphically represent the overall differences in miRNA expression between samples (Figure 2B). We subsequently performed differential expression analyses between the groups. After FDR correction for multiple testing, only one putative novel miRNA was found to be significantly downregulated (adjusted p value < 0.05) in the preclinical stage group compared with the healthy control group (Figure 2C, Additional file 5). This miRNA was predicted by miRDeep2 and has not been previously described in other species. Its precursor sequence was mapped to chromosome 7 in the *Ovis aries* genome and exhibited a characteristic stem–loop structure. The predicted MFE probability of 0.045 suggested a low likelihood of random folding, supporting its classification as a true miRNA precursor (Additional file 6).

In the comparison of the clinical stages of the scrapie and healthy control groups, 126 miRNAs were found to have an adjusted p value < 0.05 and an absolute value of $\log_2 FC > 0.8$ (Figure 2D). Among these, 60 miRNAs were predicted to be novel miRNAs by miRDeep2 (Additional file 7). The remaining 66 known miRNAs included 63 that were significantly upregulated and 3 that were significantly downregulated in clinical sheep (Additional file 8). Among the 60 miRNAs predicted as novel, 28 showed high sequence similarity (E value < 0.001) to entries in the RumimiR database, suggesting that they had been previously detected in other ruminant studies (Additional file 9).

Functional enrichment analysis highlights neurodegeneration-related pathways

To further investigate the biological processes in which significantly dysregulated miRNAs might be involved, we performed a KEGG pathway enrichment analysis
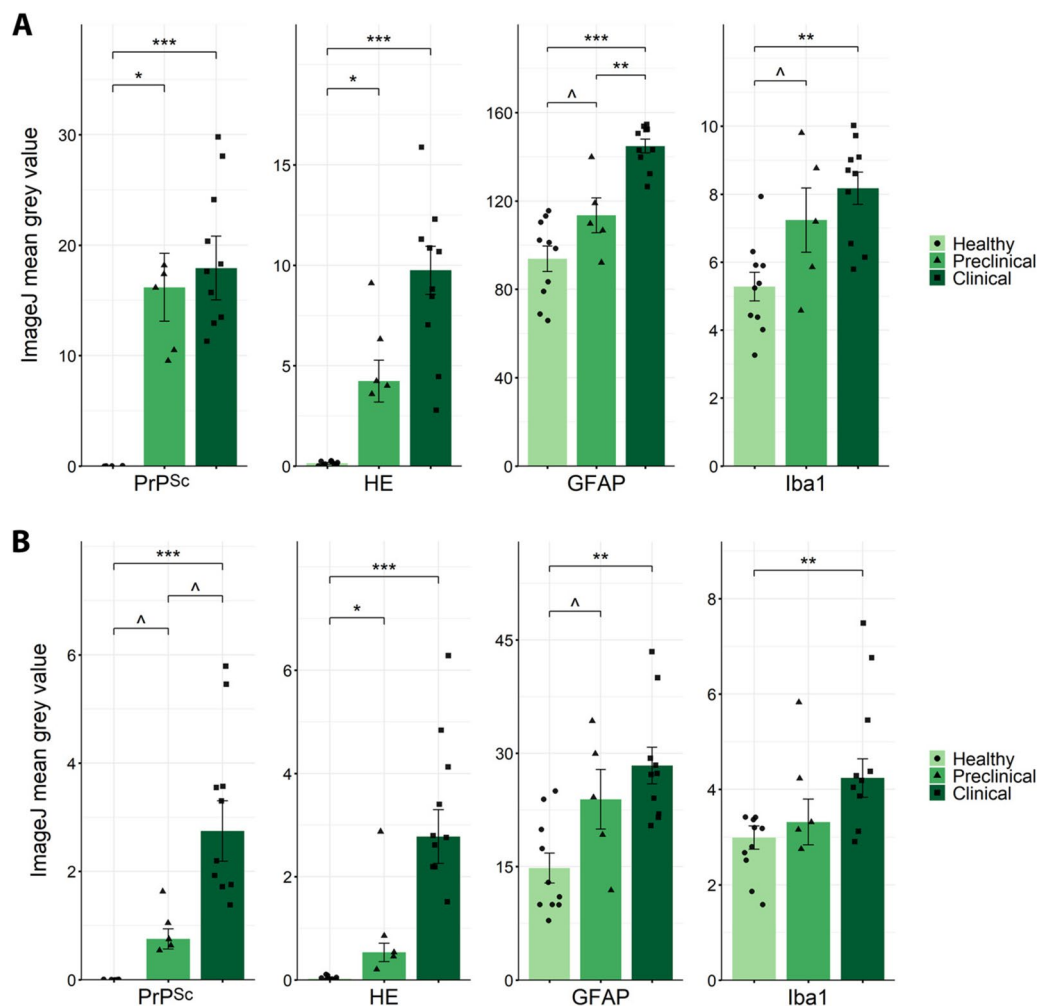
Figure 1 Neuropathological features in the obex (A) and thalamus (B). Scatter plots representing the mean grey values calculated by ImageJ, using representative microphotographs of each area and a consistent threshold for all samples in each neuropathological feature analysed: PrP^{Sc} deposits (PrP^{Sc}), spongiosis (HE), astrogliosis measured with glial fibrillary acidic protein (GFAP), and microgliosis measured using ionised calcium-binding adaptor molecule 1 (Iba1). The bars and error lines indicate the means of individual values and standard deviations or the medians and interquartile ranges for normally and non-normally distributed data, respectively. For each neuropathological feature, significant differences between healthy (light green and circles, $n = 10$) and preclinical (green and triangles, $n = 5$) and clinical (dark green and squares, $n = 10$) naturally affected scrapie groups were measured using one-way ANOVA followed by Tukey's HSD (normally distributed data) or the Kruskal–Wallis test followed by Dunn's test (non-normally distributed). *p value < 0.05, **p value < 0.01, ***p value < 0.001, ^p value < 0.1 (tendency).

using DIANA-miRPath. Among the total 66 known miRNAs significantly dysregulated in the clinical stage, only 57 miRNAs were mapped to the human miR-Path database. We obtained 85 significantly enriched KEGG pathways (adjusted p value < 0.01) after filtering for pathways with at least 55 input miRNAs involved (Additional file 10). The top 20 most significantly enriched pathways are listed in Table 1. These include proteolysis, autophagy and multiple neurodegenerative conditions.

Blood miRNA validation by RT-qPCR

To select miRNAs for RT-qPCR validation, we prioritised those that were upregulated in the clinical stage group compared with the healthy control group, since the majority (63 out of 66) of the known significantly dysregulated miRNAs identified in this comparison were overexpressed in clinical animals. Our selection criteria included greater statistical significance, a fold change in differential expression, and a median read count above 100 in both groups studied to ensure
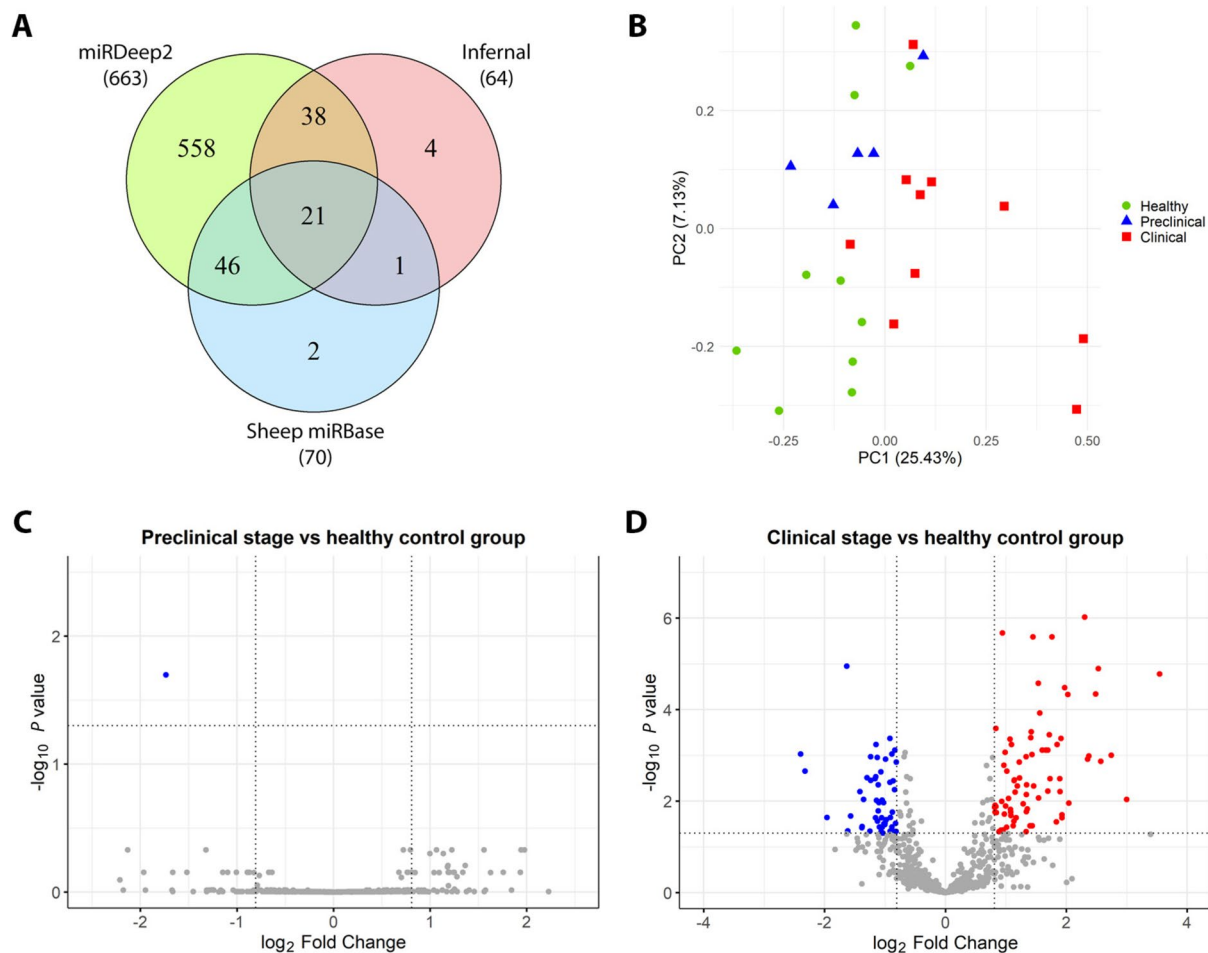
Pérez-Lázaro *et al. Veterinary Research*   (2025) 56:132

Page 8 of 18

Figure 2 Data exploration of the small RNA sequencing results. **A** Venn diagram representing miRNAs identified by miRDeep2, Infernal and sheep miRBase and their overlap after filtering the small RNA sequencing results for minimum expression levels. **B** Principal component analysis (PCA) of normalised small RNA sequencing read counts from all blood samples. The x- and y-axes represent two principal components (PC1 and PC2), which account for 25.43% and 7.13% of the variance between samples, respectively. The data points represent healthy animals (green circles, $n = 10$) and preclinical (blue triangles, $n = 5$) and clinical (red squares, $n = 10$) scrapie-affected sheep. **C and D**, Volcano plots showing differential blood miRNA expression in preclinical (**C**) and clinical stages (**D**) compared with healthy controls. The horizontal line shows an adjusted p value of 0.05, whereas the vertical lines show $\log_2$-fold change values of -0.8 and +0.8. Significantly downregulated miRNAs are coloured in blue, significantly upregulated miRNAs are coloured in red, and non-differentially expressed miRNAs are coloured in grey.

reliable detection by RT-qPCR, given the sensitivity limitations of this validation technique. On the basis of these parameters and the exploratory nature of this study, eight miRNAs were selected for further validation by RT-qPCR. Figure 3 represents a hierarchical clustering analysis with the relative expression of each of the selected miRNAs from the small RNA sequencing data. The clusters in which the samples are grouped according to the expression of the selected miRNAs in each sample resemble the groups studied.

RT-qPCR was used to measure the relative expression of the eight miRNAs in the blood of healthy, preclinical and naturally affected scrapie sheep. As represented in Fig. 4, five of these miRNAs (miR-223-3p, miR-1271-5p,

let-7f-5p, miR-186-5p and miR-425-5p) were significantly upregulated in the clinical scrapie sheep compared with the healthy animals.

Replication of blood miRNA expression in the central nervous system

Since the miRNAs found in blood can originate from different tissues in the organism, we sought to investigate whether the five significantly dysregulated miRNAs in blood were also altered in the CNS. For this purpose, we analysed their expression by RT-qPCR in the most affected areas of the CNS in naturally affected scrapie sheep: the medulla oblongata at the level of the obex (Figure 5A) and thalamus (Figure 5B).

Pérez-Lázaro *et al. Veterinary Research*   (2025) 56:132

Page 9 of 18

Table 1 Top 20 KEGG pathways associated with significantly dysregulated (adjusted *p* value < 0.01) miRNAs in blood.

KEGG pathway	adj *p* value[1]	Target genes (n)	miRNAs (n)
Ubiquitin mediated proteolysis	3.64E-19	124	56
Pathways in cancer	9.90E-17	375	56
Shigellosis	1.61E-15	200	56
Autophagy—animal	1.24E-14	120	55
Cell cycle	6.24E-13	106	56
Proteoglycans in cancer	2.56E-12	163	57
FoxO signalling pathway	4.83E-12	111	56
Renal cell carcinoma	2.31E-11	63	55
Amyotrophic lateral sclerosis	1.03E-10	270	56
Protein processing in endoplasmic reticulum	1.11E-10	143	55
Salmonella infection	2.96E-10	192	56
Pathways of neurodegeneration—multiple diseases	6.36E-10	341	56
Chronic myeloid leukemia	1.21E-09	67	56
Focal adhesion	2.71E-09	151	56
HIF-1 signalling pathway	3.95E-09	88	55
Huntington disease	5.25E-09	224	56
Colorectal cancer	5.35E-09	72	56
p53 signalling pathway	7.47E-09	63	56
Neurotrophin signalling pathway	7.47E-09	95	55
Prostate cancer	9.96E-09	80	55

[1] adj *p* value: *p* value adjusted via Benjamini–Hochberg false discovery rate correction

While we did not observe significant differences in the expression of miR-223 in either of the two areas of the CNS, the other four miRNAs presented significant increases in expression in clinical scrapie animals. Furthermore, in the obex, we observed very significant upregulation of miR-1271 (*p* value < 0.01) in preclinical animals and a close to significant tendency toward upregulation of let-7f and miR-186 (both *p* values < 0.1) in the preclinical stage of the disease compared with healthy animals.

MiRNA expression strongly correlates with neuropathological features

Having identified four miRNAs (miR-1271, let-7f, miR-186 and miR-425) significantly dysregulated in both blood and the two CNS areas studied, we sought to evaluate whether the miRNA expression levels were associated with the hallmark neuropathological features of prion diseases in the CNS: PrP^{Sc} deposits, spongiosis, astrogliosis and microgliosis. A correlation analysis was performed for each area between the RT-qPCR data from the miRNA expression in the CNS and the ImageJ scores of the neuropathological changes. Although the expression of miR-223 was not significantly altered in the CNS samples, it was included in the analysis because of its significantly altered expression in blood. As expected, miR-223 had no significant correlation with neuropathological

features in either the obex (Figure 6A) or thalamus (Figure 6B). In contrast, the other four miRNAs showed very significant correlations with all or some of the neuropathological features examined here, in both areas, confirming their potential association with disease progression in the CNS.

Significant miRNA target dysregulation in scrapie progression

Since it seems likely that miR-1271, let-7f, miR-186 and miR-425 could be directly related to prion pathology, they are most likely to affect the regulation of genes that play important roles in neurodegeneration. To explore this hypothesis further, we searched for predicted gene targets for these miRNAs. Using TarBase, miRDB and miRPath and confirming the homology of these miRNA sequences to those of humans, we selected four genes related to neurodegenerative pathways in which these four miRNAs are involved (Additional file 11): *KRAS*, *MDM2*, *CCND2* and *UBQLN2*. Additionally, we identified four other genes that are predicted to be targets of these miRNAs and have been found to be downregulated in previously published articles on scrapie-affected sheep [47, 48]: *DUSP1*, *IMMT*, *CLTC* and *PGK1*. Table 2 shows these target genes with their associated miRNAs and the pathways in which they are involved or their previously reported expression in scrapie sheep.
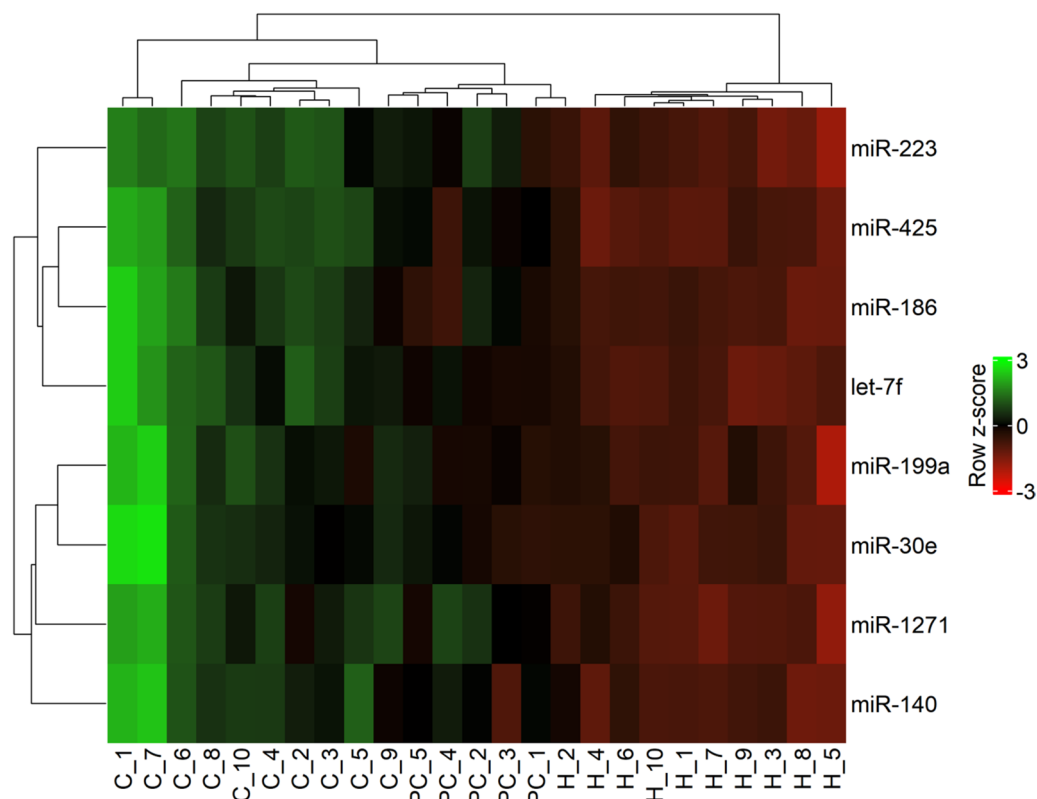
Figure 3 Hierarchical clustering analysis of selected miRNAs in blood. Relative differential expression of selected miRNAs (in rows), presented as z scores calculated from normalised small RNA sequencing read counts of all blood samples (in columns; C: clinical stage of naturally scrapie-affected sheep, PC: preclinical stage, H: healthy controls). Dendrograms in the y- and x-axes show clustering of miRNAs and samples, respectively, using a complete linkage method and the Euclidean method for distance measurement.

To further explore whether miRNAs may regulate their target expression through mRNA degradation, we analysed the expression of the target genes we predicted from significantly upregulated miRNAs using RT-qPCR in the CNS, both the obex (Figure 7A) and the thalamus (Figure 7B). In the present study, all target genes except for *DUSP1* were found to be significantly downregulated in naturally affected scrapie sheep compared with healthy sheep, which is consistent with miRNA regulation. Notably, *MDM2*, *UBQLN2* and *PGK1* were also significantly downregulated in the preclinical stage group compared with the healthy stage group, whereas *IMMT* was nearly significantly decreased (*p* value < 0.1) in the preclinical stage group. In contrast, gene expression in the thalamus showed greater variability, and significant downregulation was detected only for *KRAS* and *CLTC* in clinical scrapie animals compared with healthy controls. *UBQLN2* and *PGK1* also tended to be downregulated in the clinical stage of disease.

Discussion

The importance of miRNAs as biomarkers in body fluids for detecting disease presence or prognosis has increased in recent years. In this study, we explored circulating miRNAs in a natural model of prion disease, specifically sheep with classical scrapie, in which preclinical animals can be identified by rectal lymphoid biopsies performed in vivo. Using next-generation sequencing, we investigated for the first time differences in miRNA expression in blood from healthy animals and preclinical and clinical naturally affected classical scrapie sheep. Owing to the limited miRNA annotation for this species, we used the bioinformatic tool miRDeep2, which addresses this limitation by predicting novel and mature miRNAs on the basis of available annotations from other species. After statistical comparisons between groups, we identified one novel miRNA dysregulated in the preclinical stage and 126 miRNAs that were altered in the clinical stage of disease compared with healthy animals. Among these
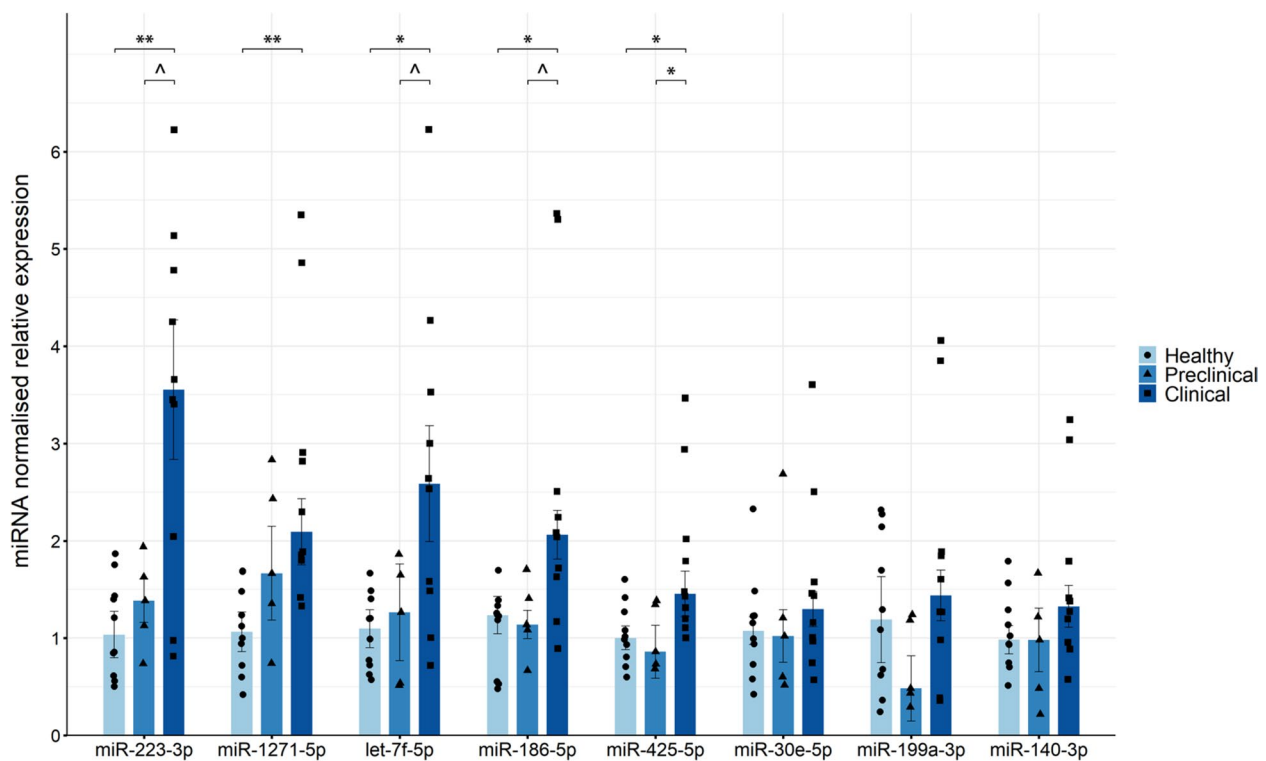
Pérez-Lázaro *et al. Veterinary Research*   (2025) 56:132

Page 11 of 18

Figure 4 Relative expression of selected miRNAs measured by RT-qPCR in blood. Grouped bar plot with overlaid scatter plot showing individual $2^{-\Delta\Delta Ct}$ values relative to the healthy group. The bars and error lines indicate the means of individual values and standard deviations or the medians and interquartile ranges for normally and non-normally distributed data, respectively. miRNA expression was normalised to the mean expression of miR-92a and miR-328. For each miRNA, significant differences between healthy (light blue and circles, $n = 10$) and preclinical (blue and triangles, $n = 5$) and clinical (dark blue and squares, $n = 10$) naturally affected scrapie groups were measured using one-way ANOVA followed by Tukey's HSD (normally distributed data) or the Kruskal–Wallis test followed by Dunn's test (non-normally distributed). $*p$ value < 0.05, $**p$ value < 0.01, $^\wedge p$ value < 0.1 (tendency).

clinically dysregulated miRNAs, five were validated in blood by RT-qPCR, and four of them were also found to be altered in the CNS. These miRNAs presented expression levels that were significantly correlated with the typical neuropathological features of prion diseases: PrP^{Sc} deposits, spongiosis and gliosis.

Overall, our sequencing results indicate that the dysregulation of circulating miRNAs in the blood predominantly begins during the clinical stage of the disease. The minor differences found in the preclinical stage of the disease may partly reflect the limited number of preclinical animals used in this study. However, our analyses of miRNA expression in the CNS, particularly in the obex, revealed a tendency toward upregulation during the preclinical stage, suggesting early, although subtle, changes in the brain prior to the onset of clinical signs. This observation implies that miRNA changes in blood occur later than those in the CNS, potentially limiting their utility as circulating biomarkers for the preclinical stage. These results in a natural model of prion disease align with other studies in murine models, where

minimal miRNA changes were observed in the CNS of preclinical animals [14, 15]. However, those studies were unable to validate their CNS sequencing findings in body fluids, such as plasma and cerebrospinal fluid. This discrepancy may suggest that the major differences in the CNS in terms of miRNA expression are not reflected in circulating fluids. In contrast, our reverse approach, beginning with blood sequencing and validating findings in the CNS, revealed that four of the five miRNAs altered in the blood were significantly dysregulated in the CNS. These findings indicate that most of the miRNA changes observed in the blood of scrapie animals likely originate from the CNS, further supporting the hypothesis that the CNS serves as a primary source for miRNA dysregulation in body fluids during the clinical stage of prion disease.

To further investigate the potential role of the dysregulated miRNAs identified in the clinical stage of the disease, we performed a KEGG pathway enrichment analysis. Several pathways related to neurodegeneration were among the top 20 significantly dysregulated pathways. Notably, we highlight autophagy,
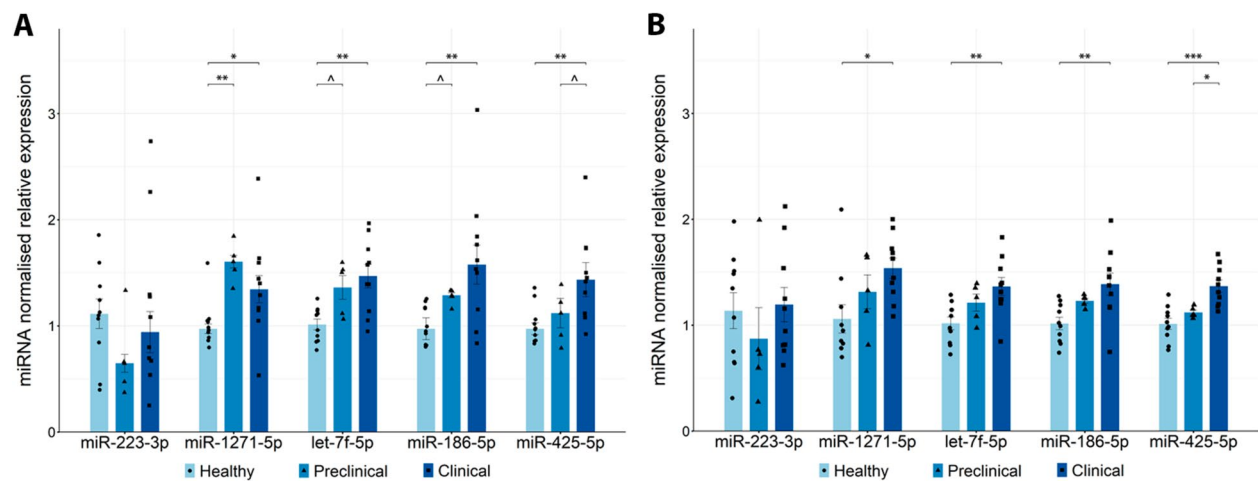
Figure 5 Relative expression of significantly dysregulated miRNAs of interest in the blood measured by RT–qPCR in the CNS, obex (A) and thalamus (B). Grouped bar plot with overlaid scatter plot showing individual $2^{-\Delta\Delta Ct}$ values relative to the healthy group. The bars and error lines indicate the means of individual values and standard deviations or the medians and interquartile ranges for normally and non-normally distributed data, respectively. miRNA expression was normalised to the mean expression of miR-92a and miR-328 in the obex and to the mean expression of sn-U6, miR-320 and miR-328 in the thalamus. For each miRNA, significant differences between healthy (light blue and circles, $n = 10$) and preclinical (blue and triangles, $n = 5$) and clinical (dark blue and squares, $n = 10$) naturally affected scrapie groups were measured using one-way ANOVA followed by Tukey's HSD (normally distributed data) or the Kruskal–Wallis test followed by Dunn's test (non-normally distributed). *p value < 0.05, **p value < 0.01, ***p value < 0.001, ^p value < 0.1 (tendency).
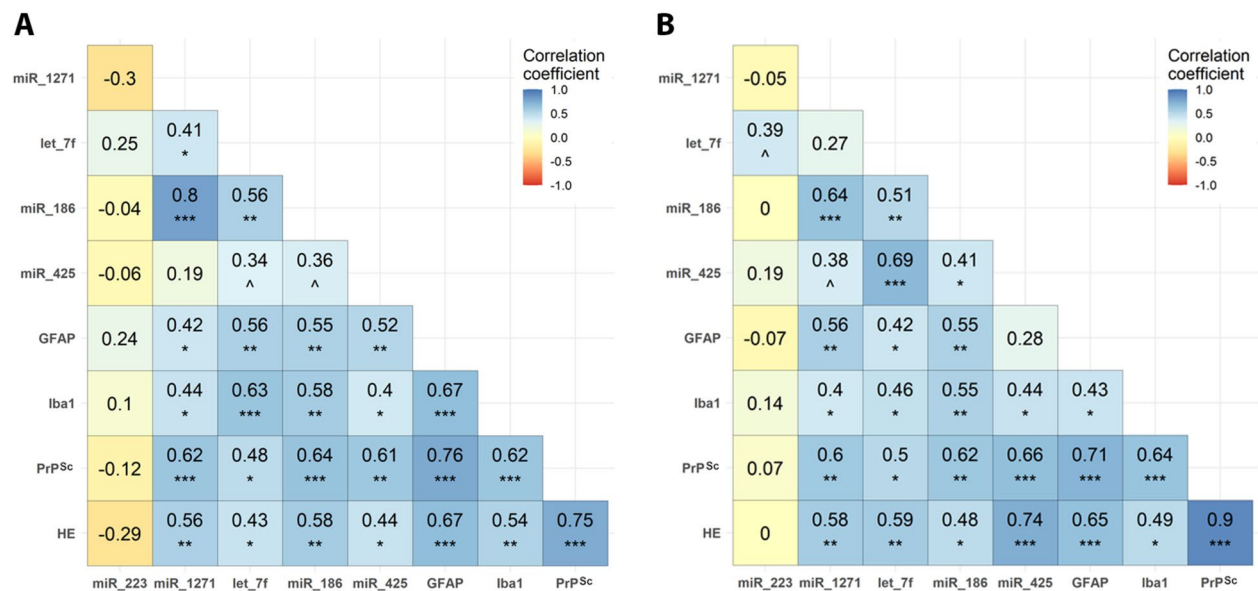

Figure 6 Correlation matrix between the miRNAs of interest and prion neuropathology in the obex (A) and thalamus (B). Spearman correlation coefficients and significance between the RT–qPCR relative expression of five miRNAs in the CNS of healthy ($n = 10$) and preclinical ($n = 5$) and clinical ($n = 10$) naturally affected scrapie sheep and their neuropathological scores: PrP^{Sc} deposits (PrP^{Sc}), spongiosis (HE), astrogliosis measured with glial fibrillary acidic protein (GFAP), and microgliosis measured using the ionised calcium-binding adaptor molecule 1 (Iba1). *p value < 0.05, **p value < 0.01, ***p value < 0.001, ^p value < 0.1 (tendency).

ubiquitin-mediated proteolysis, and protein processing in the endoplasmic reticulum pathway given their previously reported dysregulation in scrapie and other prion diseases [54, 55]. Interestingly, these pathways remained significant when the KEGG analysis was repeated using only the four miRNAs that were dysregulated in both the blood and the CNS. These findings suggest that the

Pérez-Lázaro *et al. Veterinary Research*   (2025) 56:132

Page 13 of 18

Table 2 Gene targets of the significantly dysregulated miRNAs in the CNS.

	Target gene	Gene name	miRNA[1]	Pathways[2]
Related to neurodegenerative pathways	KRAS	Kirsten rat sarcoma viral onco-gene	let-7f, miR-1271	Autophagy-animal, apoptosis, pathways of neurodegeneration-multiple diseases, foxO signalling pathway
	MDM2	Mouse double minute 2	let-7f, miR-1271, miR-186, miR-425	p53 signalling pathway, foxO signalling pathway, ubiquitin mediated proteolysis
	CCND2	Cyclin D2	let-7f, miR-186	p53 signalling pathway, foxO signalling pathway
	UBQLN2	Ubiquilin 2	let-7f, miR-186, miR-425	Protein processing in endoplasmic reticulum

	Target gene	Gene name	miRNA[1]	Expression[3]
Previously reported downregulated	DUSP1	Dual specificity phosphatase 1	let-7f	(1) FC −2.4 *p* value < 0.05
	IMMT	MICOS complex subunit MIC60	let-7f	(2) FC −0.996 *p* value < 0.01
	CLTC	Clathrin heavy chain	let-7f, miR-1271, miR-186, miR-425	(2) FC −0.839 *p* value < 0.01
	PGK1	Phosphoglycerate kinase 1	let-7f, miR-1271, miR-186	(2) FC −0.554 *p* value < 0.05

[1] Abbreviated miRNA names for hsa-let-7f-5p, hsa-miR-1271-5p, hsa-miR-186-5p, and hsa-miR-425-5p

[2] Most relevant pathways related to neurodegenerative diseases

[3] Already published $\log_2$ fold change (FC) and *p* value of these genes, in article (1) [47] or article (2) [48]. In the case of article 1, it is gene expression, whereas in the case of article 2, the expression is at the protein level. Both compare scrapie-naturally affected clinical sheep to a healthy group

selection of miRNAs for validation by RT-qPCR was representative of the broader set of altered miRNAs.

Our finding of upregulated miR-1271 in the blood and CNS, particularly in the obex during the preclinical stage, may suggest its potential early role in disease progression. There is limited research on this miRNA in neurodegenerative diseases, and it has not been previously studied in prion diseases. However, upregulation of miR-1271 has been reported in the frontal cortex and cell models of AD, which is consistent with our results [56, 57].

In contrast, let-7f has been well researched and has been linked to neuroinflammation, apoptosis and oxidative stress [58, 59]. Interestingly, let-7f has been found to be upregulated in serum from CWD animals [60], which is in accordance with our findings on the upregulation of let-7f in both the blood and CNS from scrapie-affected animals, with a nearly significant tendency toward upregulation in the obex of preclinical sheep. Moreover, other miRNAs of the let-7 family have also been found to be upregulated in exosomes from prion-infected neuronal cells and in the brains of scrapie-infected mice and sCJD patients [14, 61, 62]. In contrast, let-7f often appears to be downregulated in other neurodegenerative disorders, such as AD, PD and ALS [63–65], indicating a rather

specific and promising role for the let-7 family in prion diseases.

Interestingly, miR-186 has been researched for its potential role in regulating β-amyloid aggregation, a key feature of AD [66, 67], suggesting that it may similarly influence protein aggregation processes in prion disorders. In contrast to the upregulation of miR-186 shown in the present study, others have reported that miR-186 is downregulated in exosomes from prion-infected cells and serum from CWD cervids [60, 61]. However, a trend toward upregulation was found in the brains of scrapie-infected mice, similar to our results [62]. The overexpression of this miRNA has been linked to proapoptotic effects and reduced synaptic activity [68, 69]. Findings in AD, on the other hand, display high variability, with both up- and downregulation of miR-186 across different brain areas, indicating region-specific expression [70, 71].

Similarly, miR-425 has also been implicated in β-amyloid processing, promoting β-amyloid plaque formation [72, 73]. Although there are no previous studies of miR-425 in prion diseases, our significant finding of the upregulation of miR-425 in the blood and CNS of scrapie sheep, alongside its reported upregulation in AD blood and association with tau phosphorylation [65, 74],
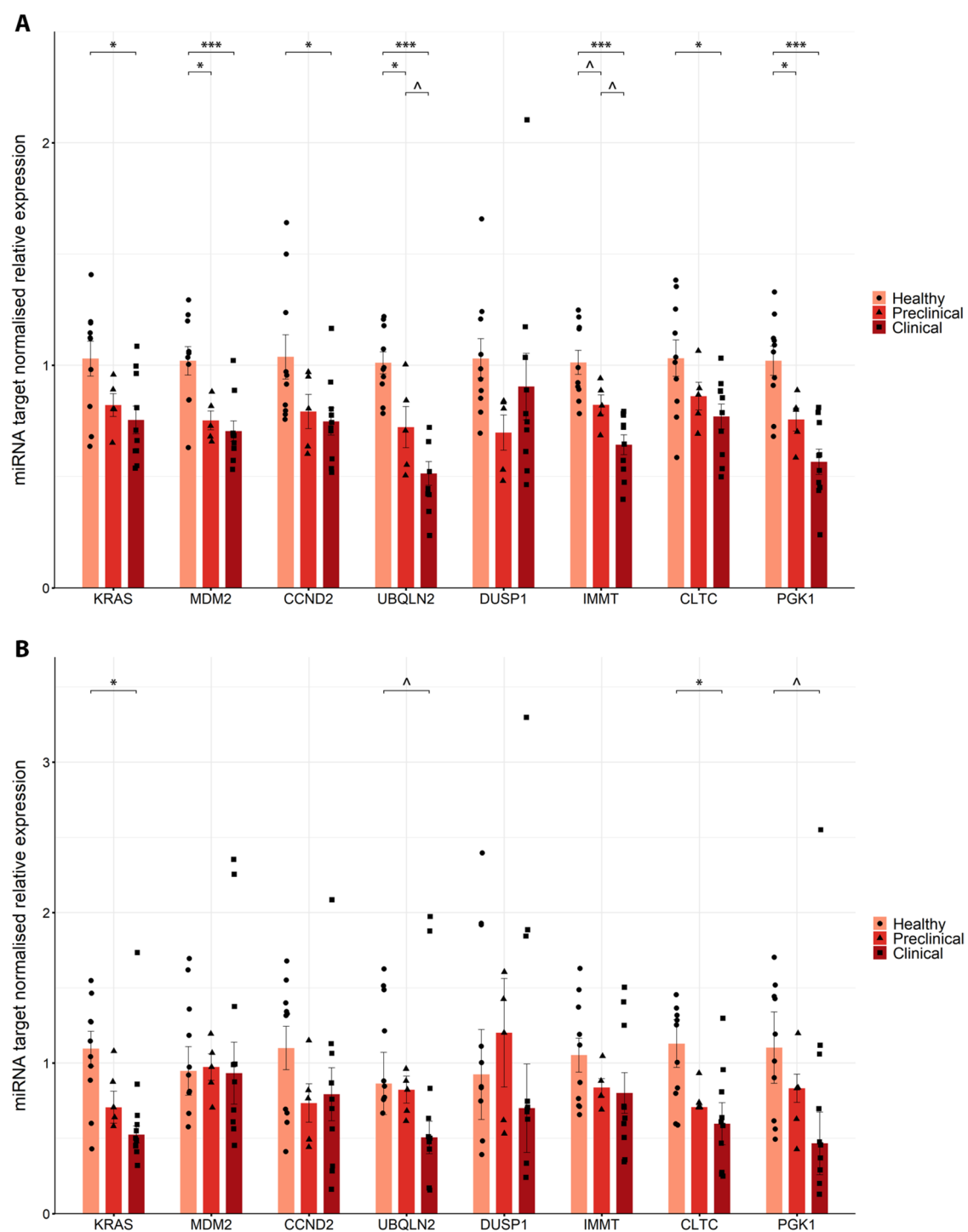
Figure 7 Relative expression of selected miRNA gene targets measured by RT-qPCR in the CNS, obex (A) and thalamus (B). Grouped bar plot with overlaid scatter plot showing individual $2^{-\Delta\Delta Ct}$ values relative to the healthy group. The bars and error lines indicate the means of individual values and standard deviations or the medians and interquartile ranges for normally and non-normally distributed data, respectively. Gene expression was normalised to the mean *G6PD* and *SDHA* in both the obex and thalamus. For each target gene, significant differences between healthy (light red and circles, *n* = 10) and preclinical (red and triangles, *n* = 5) and clinical (dark red and squares, *n* = 10) naturally affected scrapie groups were measured via one-way ANOVA followed by Tukey's HSD (normally distributed data) or the Kruskal–Wallis test followed by Dunn's test (non-normally distributed). **p* value < 0.05, ****p* value < 0.001, ^*p* value < 0.1 (tendency).

Pérez-Lázaro *et al. Veterinary Research*   (2025) 56:132

Page 15 of 18

further supports its involvement in neurotoxic protein aggregation and neurodegeneration. Conversely, miR-425 has also been found to be downregulated in AD brains and PD cell models, linking its deficiency with enhanced neuroinflammation and necroptosis [73, 75].

Overall, as shown above, considerable variability exists across studies concerning miRNA expression. As revealed by others, specific miRNAs may have opposite expression levels depending on the disease [13]. Additionally, this variability may be further influenced by differences in disease models, tissue types and methodological approaches. Therefore, caution is needed when interpreting miRNA data across different studies, especially as expression patterns may reflect the unique pathophysiology of each disorder.

Here, we selected potential target genes of these four miRNAs from the most dysregulated KEGG pathways and previous scrapie research to provide insights into their potential role in the neuropathology of prion diseases and, more specifically, of scrapie. Although we cannot confirm that the target genes identified here are regulated by the miRNAs of interest that were dysregulated in our study, owing to the lack of direct experimental validation in our samples, it is worth noting that we used highly restrictive criteria to select potential targets from previously experimentally validated miRNA–gene interactions in TarBase. Furthermore, our findings show that most of the target genes identified are downregulated, which is consistent with the expected result, since miRNAs generally act by repressing the expression of their target genes. Nonetheless, owing to the limited availability of sheep-specific genomic resources, human databases have been used to predict miRNA–target interactions. Although seed sequence conservation between sheep and humans has been confirmed, interspecies differences may compromise the accuracy of these predictions. These findings further highlight the preliminary nature of our miRNA target results and reinforce the need for future functional validation experiments in ovine samples to confirm the functional relevance of these interactions. Interestingly, the expression of *UBQLN2* and *PGK1* was significantly lower in the obex of preclinical animals than in that of healthy controls. *UBQLN2*, which is known to be involved in the degradation of misfolded proteins through the ubiquitin–proteasome system, is downregulated in AD and other neurodegenerative disorders, and mutations in this gene have been linked to ALS [76, 77]. Similarly, *PGK1* has been shown to promote autophagy and degrade pathological protein aggregates in AD [78]. While these two genes tend to be expressed only in the thalamus in the clinical stage, *KRAS* and *CLTC* downregulation was consistently significant in the clinical stage of disease in both CNS areas, and both genes have been previously reported to be downregulated in AD [79, 80]. Moreover, *CLTC* and *PGK1* protein expression has been previously reported to be downregulated in the CSF of scrapish sheep [48]. Despite some interesting findings, it is important to note the marked disparity observed between the two CNS regions analysed, as well as the difficulty in identifying a clear cumulative regulatory effect between the validated miRNAs and their predicted target genes. CNS regions may harbour distinct, potentially numerous, dysregulated miRNAs not considered in this study, which may have synergistic or tissue-specific effects on gene expression. Given these limitations, more studies should be conducted to further explore the regional variability within the CNS, which may influence the extent of miRNA-mediated gene regulation in prion diseases.

Working with the naturally occurring disease in sheep may result in greater variability in the pathological stage among animals within the same group of diseases, thus potentially hiding differences in miRNA dysregulation. However, the significant correlations observed between miRNA expression and neuropathology levels seem to overcome this limitation, supporting notable changes throughout disease progression. Moreover, the use of naturally scrapie-affected animals poses an additional challenge in identifying individuals at the preclinical stage. This resulted in a limited sample size in this group, which may reduce the statistical robustness of our findings for early-stage disease changes. Therefore, these results should be interpreted with caution and confirmed in future studies involving a larger number of animals.

In conclusion, as the first study to explore miRNA expression in blood and CNS tissues in both preclinical and clinical scrapie-affected sheep, our findings reveal widespread miRNA dysregulation, with a key validated subset consisting of miR-1271, let-7f, miR-186 and miR-425, which showed significant upregulation in the blood of clinical animals and a tendency toward significantly increased expression in the most affected brain region of preclinical sheep, correlating positively with prion neuropathology. These findings suggest that although early-stage changes in miRNA expression may be challenging to detect, miRNA dysregulation may still serve as a valuable predictor of disease progression. Given the existing variability in miRNA expression, further research is needed to clarify the specific roles of the miRNAs validated here in prion diseases and to evaluate their potential role in disease progression.

Abbreviations

AD	Alzheimer's disease
adj *p* value	adjusted *p* value
ALS	amyotrophic lateral sclerosis
bp	base pairs
cDNA	complementary DNA

Pérez-Lázaro *et al. Veterinary Research*   (2025) 56:132

Page 16 of 18

CNS	central nervous system
CSF	cerebrospinal fluid
Ct	cycle threshold
CWD	chronic wasting disease
FC	fold change
FDR	false discovery rate
GFAP	glial fibrillary acidic protein
HE	haematoxylin and eosin
Iba1	ionised calcium-binding adaptor molecule 1
IHC	immunohistochemistry
KEGG	Kyoto Encyclopedia of Genes and Genomes
MFE	minimum folding energy
miRNAs	microRNAs
mRNA	messenger RNA
PCA	principal component analysis
PD	Parkinson's disease
PrP^C	cellular prion protein
PrP^{Sc}	pathological prion protein
RIN	RNA integrity number
RISC	RNA-induced silencing complex
RT	room temperature
RT-qPCR	real-time quantitative PCR
sCJD	sporadic Creutzfeldt–Jakob disease
TSEs	transmissible spongiform encephalopathies

Supplementary Information

The online version contains supplementary material available at https://doi.org/10.1186/s13567-025-01566-0.

Additional file 1. TaqMan probes used for RT-qPCR analysis of selected and potential housekeeping miRNAs in the blood and CNS.

Additional file 2. Raw Ct values (A, C, E) and RefFinder results (B, D, F) for the housekeeping miRNAs analysed in blood (A, B), obex (C, D) and thalamus (E, F) samples. A, C and E, The means and standard deviations or medians and interquartile ranges for normally and non-normally distributed data, respectively, are shown for each group: healthy sheep (light blue circles, $n = 10$) and preclinical (blue triangles, $n = 5$) and clinical (dark blue squares, $n = 10$) naturally affected scrapie sheep. B, D and F, Overall stability rankings of candidate housekeeping miRNAs, which were calculated on the basis of the geometric means of the ranking values derived from multiple computational algorithms.

Additional file 3. Primers used for RT-qPCR analysis of potential miRNA gene targets.

Additional file 4. Raw Ct values (A, C) and RefFinder results (B, D) for the housekeeping genes analysed in obex (A, B) and thalamus (C, D) samples. A and C, Means and standard deviations or medians and interquartile ranges for normally and non-normally distributed data, respectively, are shown for each group: healthy sheep (light red circles, $n = 10$) and preclinical (red triangles, $n = 5$) and clinical (dark red squares, $n = 10$) naturally affected scrapie sheep. B and D, Overall stability rankings of candidate housekeeping genes, which are calculated on the basis of the geometric means of the ranking values derived from multiple computational algorithms.

Additional file 5. Novel significantly dysregulated miRNAs in blood from preclinical scrapie sheep compared with healthy sheep.

Additional file 6. Predicted secondary structure of the preclinical putative novel miRNA precursor. Compared with that of healthy controls, the stem–loop structure of the precursor sequence of the novel miRNA was significantly dysregulated in the preclinical stage. Each nucleotide is color-coded, representing the base-pairing probability, where values range from 0 (low probability of being base-paired) to 1 (high probability of being base-paired).

Additional file 7. Novel significantly dysregulated miRNAs in blood from clinical scrapie sheep compared with healthy sheep.

Additional file 8. Known significantly dysregulated miRNAs in blood from clinical scrapie sheep compared with healthy sheep.

Additional file 9. High similarity of novel significantly dysregulated miRNAs to previously reported miRNAs in ruminant studies.

Additional file 10. KEGG pathways involving significantly dysregulated (adjusted p value < 0.01) miRNAs in blood.

Additional file 11. KEGG pathways involving the significantly dysregulated (adjusted *p* value < 0.01) miRNAs in the CNS.

Availability of data and materials

The raw fastq.gz sequencing files and normalised read counts have been deposited in the NCBI Gene Expression Omnibus (GEO) and are accessible through GEO series accession number GSE287730.

Declarations

Ethics approval and consent to participate

All experiments involving animals were conducted following the ARRIVE guidelines and under the ethical approval granted by the Ethical Committee for Animal Experimentation of the University of Zaragoza (references PI38/15 and PI17/21). All procedures adhered to the Spanish Royal Decree 53/2013, aligned with the European Directive 2010/63 on the protection of animals used for scientific and experimental purposes.

Competing interests

The authors declare that they have no competing interests.

References

1. Castle AR, Gill AC (2017) Physiological functions of the cellular prion protein. Front Mol Biosci 4:19
2. Budka H (2003) Neuropathology of prion diseases. Br Med Bull 66:121–130
3. Uttley L, Carroll C, Wong R, Hilton DA, Stevenson M (2020) Creutzfeldt-Jakob disease: a systematic review of global incidence, prevalence, infectivity, and incubation. Lancet Infect Dis 20:e2–e10
4. Brundin P, Melki R, Kopito R (2010) Prion-like transmission of protein aggregates in neurodegenerative diseases. Nat Rev Mol Cell Biol 11:301–307
5. Polymenidou M, Cleveland DW (2011) The seeds of neurodegeneration: prion-like spreading in ALS. Cell 147:498–508

Pérez-Lázaro *et al. Veterinary Research*   (2025) 56:132

Page 17 of 18

6. Monleón E, Garza MC, Sarasa R, Álvarez-Rodriguez J, Bolea R, Monzón M, Vargas MA, Badiola JJ, Acín C (2011) An assessment of the efficiency of PrP^{Sc} detection in rectal mucosa and third-eyelid biopsies from animals infected with scrapie. Vet Microbiol 147:237–243

7. López-Pérez O, Bernal-Martín M, Hernaiz A, Llorens F, Betancor M, Otero A, Toivonen JM, Zaragoza P, Zerr I, Badiola JJ, Bolea R, Martín-Burriel I (2020) BAMBI and CHGA in prion diseases: neuropathological assessment and potential role as disease biomarkers. Biomolecules 10:706

8. Llorens F, Barrio T, Correia Â, Villar-Piqué A, Thüne K, Lange P, Badiola JJ, Schmitz M, Lachmann I, Bolea R, Zerr I (2018) Cerebrospinal fluid prion disease biomarkers in pre-clinical and clinical naturally occurring scrapie. Mol Neurobiol 55:8586–8591

9. Quinlan S, Kenny A, Medina M, Engel T, Jimenez-Mateos EM (2017) Micro-RNAs in neurodegenerative diseases. In: Galluzzi L, Vitale I (eds) MiRNAs in aging and cancer. Int Rev Cell Mol Biol, Volume 334. Elsevier, pp 309–343

10. Moreno-García L, López-Royo T, Calvo AC, Toivonen JM, de la Torre M, Moreno-Martínez L, Molina N, Aparicio P, Zaragoza P, Manzano R, Osta R (2020) Competing endogenous RNA networks as biomarkers in neurode-generative diseases. Int J Mol Sci 21:9582

11. Filipowicz W, Bhattacharyya SN, Sonenberg N (2008) Mechanisms of post-transcriptional regulation by microRNAs: are the answers in sight? Nat Rev Genet 9:102–114

12. Contiliani DF, Ribeiro YdA, de Moraes VN, Pereira TC (2021) MicroRNAs in prion diseases - from molecular mechanisms to insights in translational medicine. Cells 10:1620

13. Norsworthy PJ, Thompson AGB, Mok TH, Guntoro F, Dabin LC, Nihat A, Paterson RW, Schott JM, Collinge J, Mead S, Viré EA (2020) A blood miRNA signature associates with sporadic Creutzfeldt-Jakob disease diagnosis. Nat Commun 11:3960

14. Llorens F, Thüne K, Martí E, Kanata E, Dafou D, Díaz-Lucena D, Vivancos A, Shomroni O, Zafar S, Schmitz M, Michel U, Fernández-Borges N, Andréoletti O, Del Río JA, Díez J, Fischer A, Bonn S, Sklaviadis T, Torres JM, Ferrer I, Zerr I (2018) Regional and subtype-dependent miRNA signatures in sporadic Creutzfeldt-Jakob disease are accompanied by alterations in miRNA silencing machinery and biogenesis. PLoS Pathog 14:e1006802

15. Toivonen JM, Sanz-Rubio D, López-Pérez Ó, Marín-Moreno A, Bolea R, Osta R, Badiola JJ, Zaragoza P, Espinosa JC, Torres JM, Martín-Burriel I (2020) MicroRNA alterations in a Tg501 mouse model of prion disease. Biomolecules 10:908

16. Sanz-Rubio D, López-Pérez O, de Andrés-Pablo A, Bolea R, Osta R, Badiola JJ, Zaragoza P, Martín-Burriel I, Toivonen JM (2017) Increased circulating microRNAs miR-342-3p and miR-21-5p in natural sheep prion disease. J Gen Virol 98:305–310

17. López-Pérez O, Sanz-Rubio D, Hernaiz A, Betancor M, Otero A, Castilla J, Andréoletti O, Badiola JJ, Zaragoza P, Bolea R, Toivonen JM, Martín-Burriel I (2021) Cerebrospinal fluid and plasma small extracellular vesicles and miRNAs as biomarkers for prion diseases. Int J Mol Sci 22:6822

18. Chen X, Ba Y, Ma L, Cai X, Yin Y, Wang K, Guo J, Zhang Y, Chen J, Guo X, Li Q, Li X, Wang W, Zhang Y, Wang J, Jiang X, Xiang Y, Xu C, Zheng P, Zhang J, Li R, Zhang H, Shang X, Gong T, Ning G, Wang J, Zen K, Zhang J, Zhang CY (2008) Characterization of microRNAs in serum: a novel class of biomark-ers for diagnosis of cancer and other diseases. Cell Res 18:997–1006

19. Rayner KJ, Hennessy EJ (2013) Extracellular communication via microRNA: lipid particles have a new message. J Lipid Res 54:1174–1181

20. Cheng L, Quek C, Li X, Bellingham SA, Ellett LJ, Shambrook M, Zafar S, Zerr I, Lawson VA, Hill AF (2021) Distribution of microRNA profiles in pre-clinical and clinical forms of murine and human prion disease. Commun Biol 4:411

21. Acín C, Martín-Burriel I, Goldmann W, Lyahyai J, Monzón M, Bolea R, Smith A, Rodellar C, Badiola JJ, Zaragoza P (2004) Prion protein gene poly-morphisms in healthy and scrapie-affected Spanish sheep. J Gen Virol 85:2103–2110

22. Vargas F, Bolea R, Monleón E, Acín C, Vargas A, De Blas I, Luján L, Badiola JJ (2005) Clinical characterisation of natural scrapie in a native Spanish breed of sheep. Vet Rec 156:318–320

23. González L, Dagleish MP, Martin S, Dexter G, Steele P, Finlayson J, Jeffrey M (2008) Diagnosis of preclinical scrapie in live sheep by the immunohisto-chemical examination of rectal biopsies. Vet Rec 162:397–403

24. Monleón E, Monzón M, Hortells P, Vargas A, Acín C, Badiola JJ (2004) Detection of PrP^{Sc} on lymphoid tissues from naturally affected scrapie animals: comparison of three visualization systems. J Histochem Cyto-chem 52:145–151

25. Guijarro IM, Garcés M, Andrés-Benito P, Marín B, Otero A, Barrio T, Car-mona M, Ferrer I, Badiola JJ, Monzón M (2020) Assessment of glial activa-tion response in the progress of natural scrapie after chronic dexametha-sone treatment. Int J Mol Sci 21:3231

26. Landini G, Martinelli G, Piccinini F (2021) Colour deconvolution: stain unmixing in histological imaging. Bioinformatics 37:1485–1487

27. Crowe AR, Yue W (2019) Semi-quantitative determination of protein expression using immunohistochemistry staining and analysis: an inte-grated protocol. Bio Protoc 9:e3465

28. Andrews S (2010) FastQC: a quality control tool for high throughput sequence data. https://www.bioinformatics.babraham.ac.uk/projects/fastqc/. Accessed 11 Apr 2022

29. Jiang H, Lei R, Ding S-W, Zhu S (2014) Skewer: a fast and accurate adapter trimmer for next-generation sequencing paired-end reads. BMC Bioin-form 15:182

30. Axtell MJ (2013) ShortStack: comprehensive annotation and quantifica-tion of small RNA genes. RNA 19:740–751

31. Langmead B, Trapnell C, Pop M, Salzberg SL (2009) Ultrafast and memory-efficient alignment of short DNA sequences to the human genome. Genome Biol 10:R25

32. Kozomara A, Birgaoanu M, Griffiths-Jones S (2019) miRBase: from micro-RNA sequences to function. Nucleic Acids Res 47:D155–D162

33. Anders S, Pyl PT, Huber W (2015) HTSeq-a Python framework to work with high-throughput sequencing data. Bioinformatics 31:166–169

34. Nawrocki EP, Eddy SR (2013) Infernal 1.1: 100-fold faster RNA homology searches. Bioinformatics 29:2933–2935

35. Kalvari I, Nawrocki EP, Ontiveros-Palacios N, Argasinska J, Lamkiewicz K, Marz M, Griffiths-Jones S, Toffano-Nioche C, Gautheret D, Weinberg Z, Rivas E, Eddy SR, Finn RD, Bateman A, Petrov AI (2021) Rfam 14: expanded coverage of metagenomic, viral and microRNA families. Nucleic Acids Res 49:D192–D200

36. Friedländer MR, Mackowiak SD, Li N, Chen W, Rajewsky N (2012) miR-Deep2 accurately identifies known and hundreds of novel microRNA genes in seven animal clades. Nucleic Acids Res 40:37–52

37. Lorenz R, Bernhart SH, Höner zu Siederdissen C, Tafer H, Flamm C, Stadler PF, Hofacker IL (2011) ViennaRNA Package 2.0. Algorithms Mol Biol 6:26

38. Bonnet E, Wuyts J, Rouze P, Van de Peer Y (2004) Evidence that microRNA precursors, unlike other non-coding RNAs, have lower folding free ener-gies than random sequences. Bioinformatics 20:2911–2917

39. Quinlan AR, Hall IM (2010) BEDTools: a flexible suite of utilities for compar-ing genomic features. Bioinformatics 26:841–842

40. Love MI, Huber W, Anders S (2014) Moderated estimation of fold change and dispersion for RNA-seq data with DESeq2. Genome Biol 15:550

41. Bourdon C, Bardou P, Aujean E, Le Guillou S, Tosser-Klopp G, Le Provost F (2019) RumimiR: a detailed microRNA database focused on ruminant spe-cies. Database (Oxford) 2019:baz099

42. Tastsoglou S, Skoufos G, Miliotis M, Karagkouni D, Koutsoukos I, Kara-vangeli A, Kardaras FS, Hatzigeorgiou AG (2023) DIANA-miRPath v4.0: expanding target-based miRNA functional analysis in cell-type and tissue contexts. Nucleic Acids Res 51:W154–W159

43. Xie F, Wang J, Zhang B (2023) RefFinder: a web-based tool for com-prehensively analyzing and identifying reference genes. Funct Integr Genomics 23:125

44. Livak KJ, Schmittgen TD (2001) Analysis of relative gene expression data using real-time quantitative PCR and the 2(-Delta Delta Ct) method. Methods 25:402–408

45. Skoufos G, Kakoulidis P, Tastsoglou S, Zacharopoulou E, Kotsira V, Miliotis M, Mavromati G, Grigoriadis D, Zioga M, Velli A, Koutou I, Karagkouni D, Stavropoulos S, Kardaras FS, Lifousi A, Vavalou E, Ovsepian A, Skoulakis A, Tasoulis SK, Georgakopoulos SV, Plagianakos VP, Hatzigeorgiou AG (2024) TarBase-v9.0 extends experimentally supported miRNA-gene interactions to cell-types and virally encoded miRNAs. Nucleic Acids Res 52:D304–D310

46. Chen Y, Wang X (2020) miRDB: an online database for prediction of func-tional microRNA targets. Nucleic Acids Res 48:D127–D131

47. Filali H, Martin-Burriel I, Harders F, Varona L, Lyahyai J, Zaragoza P, Pumarola M, Badiola JJ, Bossers A, Bolea R (2011) Gene expression profil-ing and association with prion-related lesions in the medulla oblongata of symptomatic natural scrapie animals. PLoS One 6:e19909

48. Pérez-Lázaro S, Barrio T, Bravo SB, Sevilla E, Otero A, Chantada-Vázquez MdP, Martín-Burriel I, Requena JR, Badiola JJ, Bolea R (2024) New preclinical biomarkers for prion diseases in the cerebrospinal fluid proteome revealed by mass spectrometry. Vet Q 44:1–15

49. Herrero J, Muffato M, Beal K, Fitzgerald S, Gordon L, Pignatelli M, Vilella AJ, Searle SM, Amode R, Brent S, Spooner W, Kulesha E, Yates A, Flicek P (2016) Ensembl comparative genomics resources. Database (Oxford) 2016:bav096

50. Untergasser A, Cutcutache I, Koressaar T, Ye J, Faircloth BC, Remm M, Rozen SG (2012) Primer3-new capabilities and interfaces. Nucleic Acids Res 40:e115

51. Ye J, Coulouris G, Zaretskaya I, Cutcutache I, Rozen S, Madden TL (2012) Primer-BLAST: a tool to design target-specific primers for polymerase chain reaction. BMC Bioinform 13:134

52. Lyahyai J, Serrano C, Ranera B, Badiola JJ, Zaragoza P, Martin-Burriel I (2010) Effect of scrapie on the stability of housekeeping genes. Anim Biotechnol 21:1–13

53. Betancor M, Pérez-Lázaro S, Otero A, Marín B, Martín-Burriel I, Blennow K, Badiola JJ, Zetterberg H, Bolea R (2022) Neurogranin and Neurofilament Light Chain as preclinical biomarkers in scrapie. Int J Mol Sci 23:7182

54. López-Pérez O, Badiola JJ, Bolea R, Ferrer I, Llorens F, Martín-Burriel I (2020) An update on autophagy in prion diseases. Front Bioeng Biotechnol 8:975

55. Lozada Ortiz J, Betancor M, Pérez Lázaro S, Bolea R, Badiola JJ, Otero A (2023) Endoplasmic reticulum stress and ubiquitin-proteasome system impairment in natural scrapie. Front Mol Neurosci 16:1175364

56. Majumder P, Chanda K, Das D, Singh BK, Chakrabarti P, Jana NR, Mukhopadhyay D (2021) A nexus of miR-1271, PAX4 and ALK/RYK influences the cytoskeletal architectures in Alzheimer's disease and type 2 diabetes. Biochem J 478:3297–3317

57. Xiao MF, Xu D, Craig MT, Pelkey KA, Chien CC, Shi Y, Zhang J, Resnick S, Pletnikova O, Salmon D, Brewer J, Edland S, Wegiel J, Tycko B, Savonenko A, Reeves RH, Troncoso JC, McBain CJ, Galasko D, Worley PF (2017) NPTX2 and cognitive dysfunction in Alzheimer's disease. Elife 6:e23798

58. Li K, Wang Z-Q, Zhang J-L, Lv P-Y (2020) MicroRNA let-7f protects against H2O2-induced oxidative damage in neuroblastoma cells by targeting AKT-2. Arch Med Sci 21:648–657

59. Tan W, Gu Z, Leng J, Zou X, Chen H, Min F, Zhou W, Zhang L, Li G (2019) Let-7f-5p ameliorates inflammation by targeting NLRP3 in bone marrow-derived mesenchymal stem cells in patients with systemic lupus erythematosus. Biomed Pharmacother 118:109313

60. Slota JA, Medina SJ, Klassen M, Gorski D, Mesa CM, Robertson C, Mitchell G, Coulthart MB, Pritzkow S, Soto C, Booth SA (2019) Identification of circulating microRNA signatures as potential biomarkers in the serum of elk infected with chronic wasting disease. Sci Rep 9:19705

61. Bellingham SA, Coleman BM, Hill AF (2012) Small RNA deep sequencing reveals a distinct miRNA signature released in exosomes from prion-infected neuronal cells. Nucleic Acids Res 40:10937–10949

62. Saba R, Goodman CD, Huzarewich RL, Robertson C, Booth SA (2008) A miRNA signature of prion induced neurodegeneration. PLoS One 3:e3652

63. Chen L, Yang J, Lu J, Cao S, Zhao Q, Yu Z (2018) Identification of aberrant circulating miRNAs in Parkinson's disease plasma samples. Brain Behav 8:e00941

64. Daneshafrooz N, Joghataei MT, Mehdizadeh M, Alavi A, Barati M, Panahi B, Teimourian S, Zamani B (2022) Identification of let-7f and miR-338 as plasma-based biomarkers for sporadic amyotrophic lateral sclerosis using meta-analysis and empirical validation. Sci Rep 12:1373

65. Satoh J, Kino Y, Niida S (2015) MicroRNA-Seq data analysis pipeline to identify blood biomarkers for Alzheimer's disease from public data. Biomark Insights 10:21–31

66. Kim J, Yoon H, Chung DE, Brown JL, Belmonte KC, Kim J (2016) miR-186 is decreased in aged brain and suppresses BACE1 expression. J Neurochem 137:436–445

67. Delay C, Dorval V, Fok A, Grenier-Boley B, Lambert JC, Hsiung GY, Hébert SS (2014) MicroRNAs targeting Nicastrin regulate Abeta production and are affected by target site polymorphisms. Front Mol Neurosci 7:67

68. Huang P, Wan Z, Qu S (2024) Targeting the RUNX3-miR-186-3p-DAT-IGF1R axis as a therapeutic strategy in a Parkinson's disease model. J Transl Med 22:719

69. Silva MM, Rodrigues B, Fernandes J, Santos SD, Carreto L, Santos MAS, Pinheiro P, Carvalho AL (2019) MicroRNA-186-5p controls GluA2 surface expression and synaptic scaling in hippocampal neurons. Proc Natl Acad Sci U S A 116:5727–5736

70. Wang WX, Huang Q, Hu Y, Stromberg AJ, Nelson PT (2011) Patterns of microRNA expression in normal and early Alzheimer's disease human temporal cortex: white matter versus gray matter. Acta Neuropathol 121:193–205

71. Lau P, Bossers K, Janky R, Salta E, Frigerio CS, Barbash S, Rothman R, Sierksma AS, Thathiah A, Greenberg D, Papadopoulou AS, Achsel T, Ayoubi T, Soreq H, Verhaagen J, Swaab DF, Aerts S, De Strooper B (2013) Alteration of the microRNA network during the progression of Alzheimer's disease. EMBO Mol Med 5:1613–1634

72. Ren RJ, Zhang YF, Dammer EB, Zhou Y, Wang LL, Liu XH, Feng BL, Jiang GX, Chen SD, Wang G, Cheng Q (2016) Peripheral blood microRNA expression profiles in Alzheimer's disease: screening, validation, association with clinical phenotype and implications for molecular mechanism. Mol Neurobiol 53:5772–5781

73. Hu YB, Zhang YF, Ren RJ, Dammer EB, Xie XY, Chen SW, Huang Q, Huang WY, Zhang R, Chen HZ, Wang H, Wang G (2021) MicroRNA-425 loss mediates amyloid plaque microenvironment heterogeneity and promotes neurodegenerative pathologies. Aging Cell 20:e13454

74. Yuan J, Wu Y, Li L, Liu C (2020) MicroRNA-425-5p promotes tau phosphorylation and cell apoptosis in Alzheimer's disease by targeting heat shock protein B8. J Neural Transm 127:339–346

75. Hu YB, Zhang YF, Wang H, Ren RJ, Cui HL, Huang WY, Cheng Q, Chen HZ, Wang G (2019) miR-425 deficiency promotes necroptosis and dopaminergic neurodegeneration in Parkinson's disease. Cell Death Dis 10:589

76. Longobardi A, Catania M, Geviti A, Salvi E, Vecchi ER, Bellini S, Saraceno C, Nicsanu R, Squitti R, Binetti G, Di Fede G, Ghidoni R (2024) Autophagy markers are altered in Alzheimer's disease, dementia with Lewy bodies and frontotemporal dementia. Int J Mol Sci 25:1125

77. Renaud L, Picher-Martel V, Codron P, Julien JP (2019) Key role of UBQLN2 in pathogenesis of amyotrophic lateral sclerosis and frontotemporal dementia. Acta Neuropathol Commun 7:103

78. Chen H, Li Y, Gao J, Cheng Q, Liu L, Cai R (2023) Activation of Pgk1 results in reduced protein aggregation in diverse neurodegenerative conditions. Mol Neurobiol 60:5090–5101

79. Qian XH, Liu XL, Chen SD, Tang HD (2022) Identification of immune hub genes associated with Braak stages in Alzheimer's disease and their correlation of immune infiltration. Front Aging Neurosci 14:887168

80. Canchi S, Raao B, Masliah D, Rosenthal SB, Sasik R, Fisch KM, De Jager PL, Bennett DA, Rissman RA (2019) Integrating gene and protein expression reveals perturbed functional networks in Alzheimer's disease. Cell Rep 28:1103-1116.e4

Publisher's Note